

Vertical Electrical Sounding of Water-Bearing Sub-Surface of Issele-Azagba in Southern Nigeria

Ruth E. Iserhien-Emekeme

Department of Physics, Delta State University, Abraka, Nigeria

Email: ruth.emekeme1@gmail.com

Received 4 July 2014; revised 7 August 2014; accepted 21 August 2014

Copyright © 2014 by author and Scientific Research Publishing Inc.

This work is licensed under the Creative Commons Attribution International License (CC BY).

<http://creativecommons.org/licenses/by/4.0/>



Open Access

Abstract

An electrical resistivity survey involving vertical electrical sounding (VES) technique was carried out in Issele-Azagba, Aniocha North Local Government Area of Delta State, Nigeria. This was aimed at investigating the lithologic boundaries and classification of the various subsurface formations. The data obtained were subjected to a twofold interpretative procedure involving initial partial curve matching and computer iteration. Results showed that a maximum of five subsurface layers was delineated from the geoelectric sections. This is made up of loamy topsoil underlain by relatively continuous sandy units composed of different compaction, wetness and clay content. The result also showed that the fifth substratum of the geoelectric section was the aquiferous sand relevant in groundwater development within the study area. Analysis of the result had shown that the aquifers identified in this study were vulnerable contamination percolating from the surface due to the absence of a protective aquitards.

Keywords

Issele-Azagba, Vertical Electrical Sounding, Aquifer, Resistivity Method, Geophysical Survey

1. Introduction

Geophysical surveys as a tool in geophysics are useful for a range of applications. These include geological mapping of groundwater resources, characterization of aquifer structure and the investigation of the presence or absence of protective aquitards. Other applications involve environmental mapping and monitoring of contamination, evaluation of soil moisture and salinity, and the monitoring of hazardous waste disposal sites [1]. Sub-surface soil characterization is useful for determining soil strength. The information obtained from soil characte-

rizations for instance present invaluable requirement for the foundation design of important civil engineering structures and for mineral exploration. Soil characterization using electrical measurements can be translated into useful geological and geophysical information in terms of electrical properties of subsurface soil [2] [3].

The matrix minerals in rocks are insulators and the ground resistivity is a function of various geological parameters such as the degree of saturation, the resistivity of the pore fluid, porosity, and the size of the rock particles. Others include the thickness of diffuse double layers, ion concentration and pore water [4]-[7]. Some of these factors are known to directly or indirectly correlate with others. The resistivity of dry sand is of the order of $10^5 \Omega\text{m}$ whereas the resistivity of wet sand is of the order of $10 \Omega\text{m}$. This is because natural pore water has a higher resistivity than that of solids and air. For a soil with relatively low resistivity, the electric current flows in most cases through the water. This is an indication that the resistivity of the sand depends mostly on the porosity of the medium and the resistivity of the pore fluid.

The electrical properties of clay for instance are more complicated in terms of fabric. This is because the diffuse double layer formed on and between the particles may show different conductivity from the free pore water [8] [9]. Thus, the resistivity of clay is lower than that of the resistivity of pore fluid due to the relatively high conductivity between solid and liquid interface.

The high contrast in the resistivity values of carbonate rock and clayey soil favors the use of resistivity method to quickly and economically delineate the different rock layers and obtain vertical and horizontal sedimentological information about the shallow subsurface [10]-[12].

This study is therefore aimed at using resistivity to investigate the structure of the soil and obtain the lithological boundaries and classification of the various subsurface formations in Issele-Azagba. This will provide important information for groundwater resources in order to meet the anticipated increase in demand for water in the study area.

Geology and Stratigraphy of the Study Area

Issele-Azagba is in Aniocha North Local Government area of Delta State, Nigeria and lies within latitude $6^\circ 15'N$ and $6^\circ 17'N$ and longitude $6^\circ 35'E$ and $6^\circ 40'E$ (Figure 1). This study area is fairly flat and characterized by thin to thick forest vegetation. The area lies within the Southern Nigerian Sedimentary Basin which began during the Early Cretaceous (Albian) following the basement subsidence along the Benue and Niger Troughs [13] [14]. Folding and uplift occurred in the Santonian along a northeast-southwest trending axis in the Abakaliki-Benue area. The Anambra platform lying to the west and the southwest of the Abakaliki folded belts subsided to form the Anambra Basin [15] [16].

The upper cretaceous stratigraphic succession in the Anambra Basin began with the deposition of sediments from the marine Campanian-Maastrichtian Enugu/Nkporoshales and their lateral equivalent-deltaic Owelli sandstone (Table 1). These base units were successively overlain by the lower-middle Maastrichtian deltaic coal bearing Mamu formation (lower coal measures) and middle Maastrichtian tidal Ajali sandstone (false-bedded sandstones). It is overlain by the fluvial-deltaic Nsukka formation (upper coal measures). The Imo and Nsukka formations marine shales were deposited during the Paleocene era and overlain by the regressive Ameki formation (Eocene); the paralic Ogwashi-Asaba formation (Oligocene-Miocene) was capped by the continental Benin formation (Miocene-recent) constituting the tertiary succession (Figure 1 and Figure 2). The Ogwashi-Asaba formation consists of a succession of coarse-grained sandstone, clay and carbonaceous shale, containing continental lignite seam intercalations [17] [18]. The lignite seams found within the Ogwashi-Asaba formation is usually brownish to black, varying in thickness from a few millimetres to a maximum of 6 meters.

The only river in the near vicinity of Issele-Azagba is River Osuoko which is about 7 km north of the town.

2. Methodology

2.1. Field Technique

The direct current (DC) resistivity method employs very low-frequency alternating currents (AC) as source signals for the determination of subsurface resistivity distributions [20]. The Maxwell's equations for electrostatics field will in this instance reduce to:

$$\nabla \cdot \mathbf{E} = \frac{1}{\epsilon_0} q, \quad (1)$$

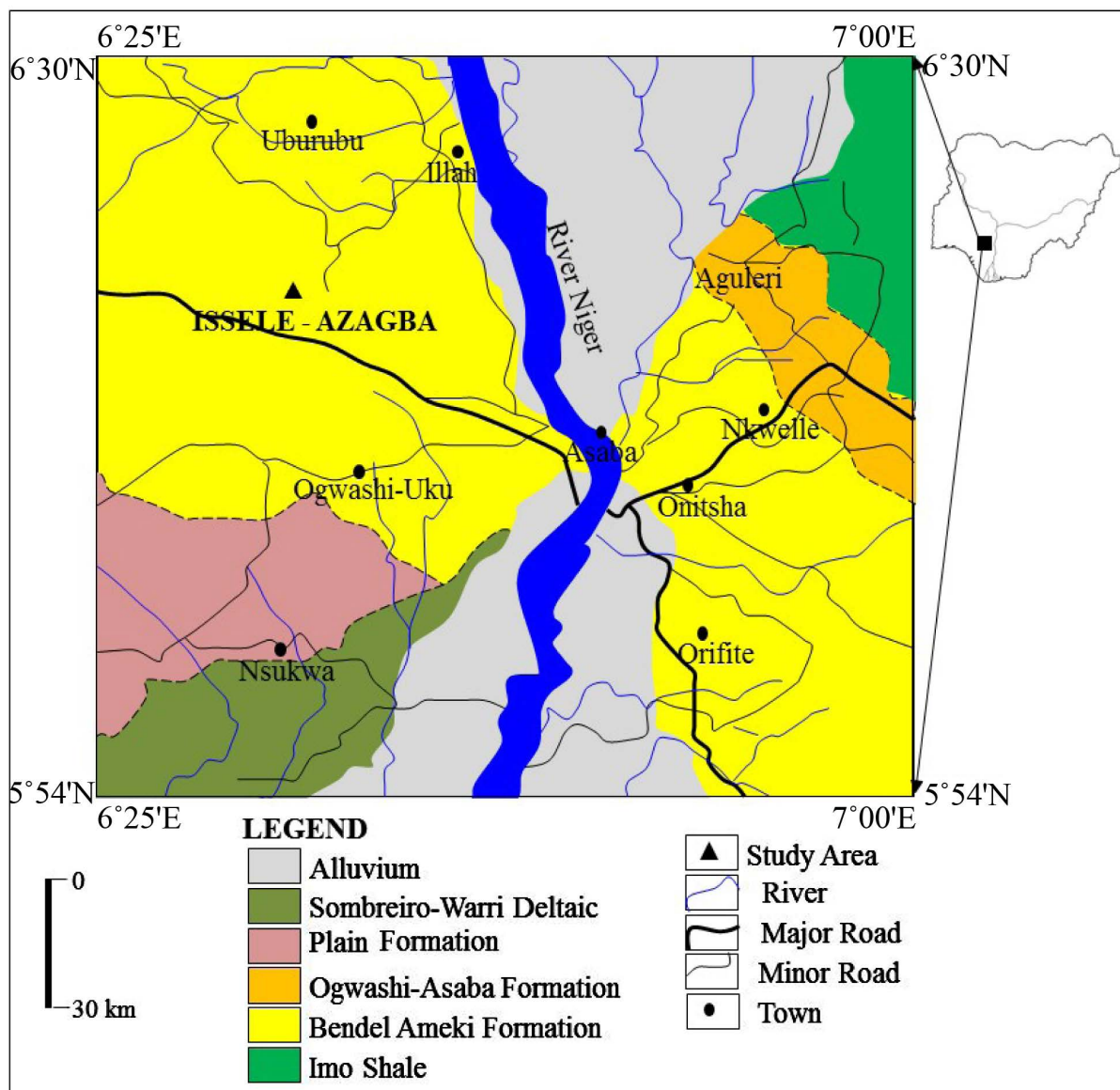


Figure 1. Map of Nigeria showing the location of Ogwashi-Asaba Formation (modified after Ogala, 2012 [19]).

Table 1. Geologic units of the Niger Delta and Anambra Basin.

Formation	Lithology	Age	Basin
Benin Formation	Coarse to medium sand with subordinate silt and clay lenses.		
Ogwashi Asaba Formation	Clay, Shales, Sandstones and Lignite	Tertiary	Niger Delta
Ameki Formation/Nanka Sand	Sandstones, Clay, Shales, Limestone		
Imo Formation	Shale		
Nsukka Formation	Sand, clay, and silt or lignite, Coals, Limestone		
Ajali Formation	Sandstones, Claystones	Cretaceous	Anambra
Mamu Formation	Coal with clastic sediments		
Enugu/Nkporo/Owelli Formation	Shales, Sandstones, Clay, Ironstones, Siltstones		

$$\nabla \times \mathbf{E} = 0, \tag{2}$$

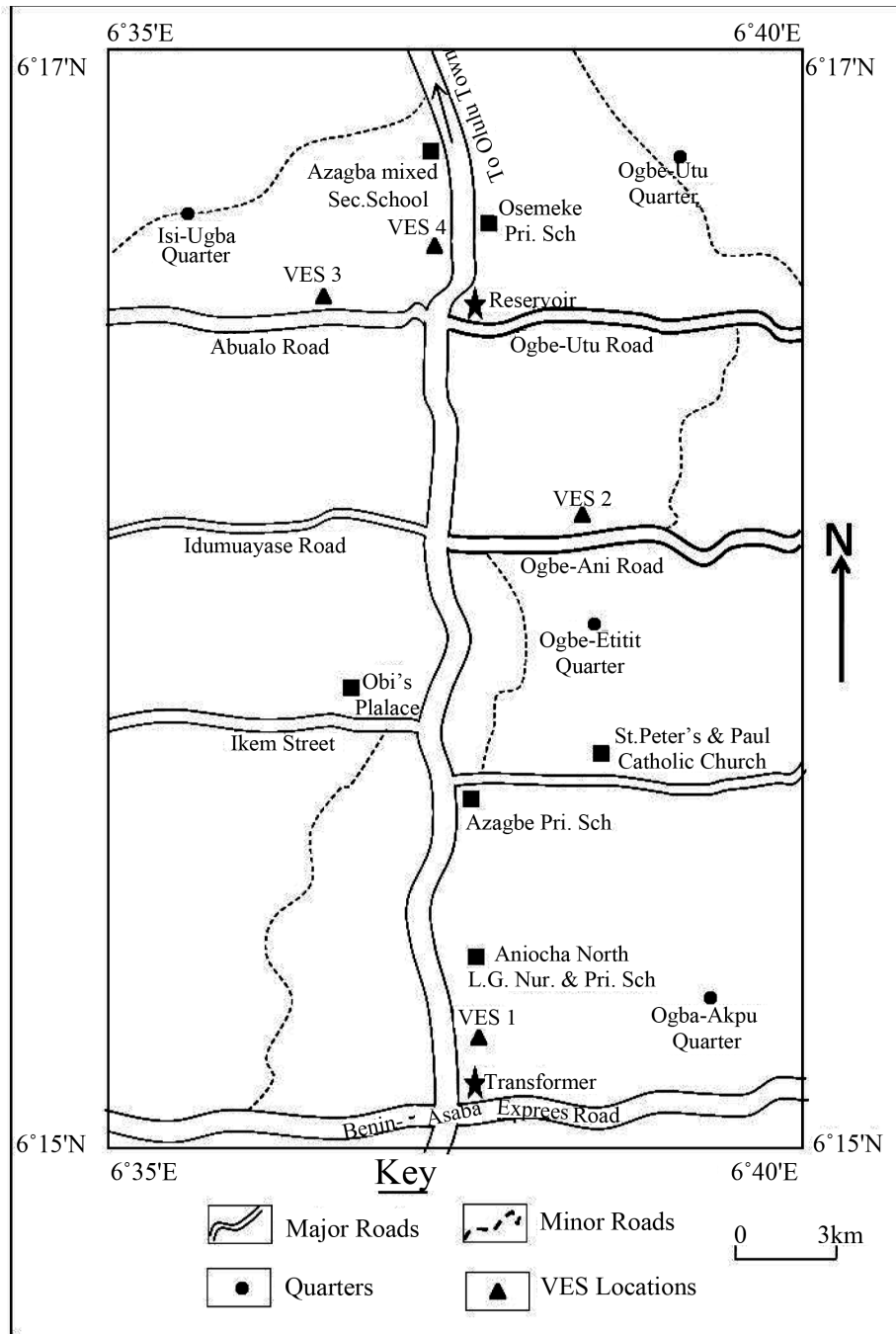


Figure 2. Location map of Issele-Azagba Town showing VES points.

where E is the electric field vector in V/m, ϵ_0 is the permittivity of free space and q is the charge density in C/m^3 . The electrostatic field can be described by the gradient of the electric potential U :

$$E = -\nabla U \tag{3}$$

Since U is usually in 3-dimension, combining Equations (1) and (3) results in the fundamental Poisson equation for electrostatic fields:

$$\nabla^2 U(x, y, z) = -\frac{1}{\epsilon_0} q(x, y, z). \tag{4}$$

The equation of continuity for a point in 3D space defined by the Dirac delta function is:

$$\nabla \cdot \mathbf{j}(x, y, z, t) = -\frac{\partial q(x, y, z, t)}{\partial t} \delta(x) \delta(y) \delta(z) \quad (5)$$

where \mathbf{j} is the current density vector and t is time. Together with Equation (3) and Ohm's law:

$$\mathbf{j} = \sigma \mathbf{E} = \frac{\mathbf{E}}{\rho}, \quad (6)$$

Equation (5) can be rearranged to:

$$-\nabla \cdot [\sigma(x, y, z) \nabla U(x, y, z)] = \frac{\partial q(x, y, z, t)}{\partial t} \delta(x - x_s) \delta(y - y_s) \delta(z - z_s), \quad (7)$$

where x_s, y_s and z_s define a point source of injected charge. The source term in Equation (7) can be rewritten in a more practical form by considering an elemental ΔV volume about the charge injection point:

$$\frac{\partial q(x, y, z, t)}{\partial t} \delta(x - x_s) \delta(y - y_s) \delta(z - z_s) = \frac{I}{\Delta V} \delta(x - x_s) \delta(y - y_s) \delta(z - z_s) \quad (8)$$

Here, I is the current driven by a point source. Substituting Equation (8) into (7) results in a partial differential equation for the electric potential in an isotropic non-uniform 3D medium generated by a point source as shown in Equation (9):

$$-\nabla \cdot [\sigma(x, y, z) \nabla U(x, y, z)] = \frac{I}{\Delta V} \delta(x - x_s) \delta(y - y_s) \delta(z - z_s). \quad (9)$$

Integrating the equation of continuity (Equation (5)) over a volume and applying Gauss' divergence theorem results in a surface integral of the current density \mathbf{j} . Substituting \mathbf{j} from Ohm's law and integrating over the surface of a sphere with radius r yields:

$$\mathbf{E}(r) = \frac{I\rho}{4\pi r^2}, \quad (10)$$

from which it is easy to show that:

$$U(r) = \frac{I\rho}{4\pi r}. \quad (11)$$

Equation (11) describes the potential due to a single point source within a homogenous space at a distance r from the injection point. For the homogenous half-space.

$$U(r) = \frac{I\rho}{2\pi r} \quad (12)$$

Given two current electrodes A and B as shown in **Figure 3** and applying Equation (12), the potential at arbitrary point M is:

$$U_M = \frac{I\rho}{2\pi} \left[\frac{1}{r_1} - \frac{1}{r_2} \right] \quad (13)$$

where r_1 is the distance between M and A and r_2 the distance between M and B.

To measure potential differences, two electrodes are needed. Theoretically, the injecting electrodes A and B could be used to measure the response signal. However, transition resistances between the electrodes and the subsurface would influence the measurements in an unknown fashion [21]. A dedicated pair of electrodes for measuring voltage differences completes the four-electrode array commonly used in DC resistivity surveys. Subtracting the potential at point N from that at point M gives the potential difference ΔU between M and N:

$$\Delta U = \frac{I\rho}{2\pi} \left[\frac{1}{r_1} - \frac{1}{r_2} - \frac{1}{r_3} + \frac{1}{r_4} \right] = \frac{I\rho}{K} \quad (14)$$

where r_3 is the distance between N and A and r_4 the distance between N and B. Since K only contains the

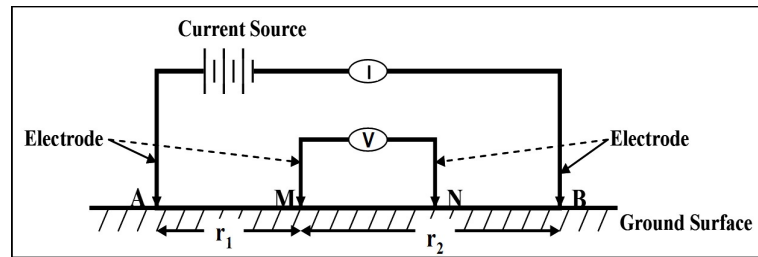


Figure 3. Schematic diagram of a four-point Schlumberger Array. A and B are current electrodes, M and N are potential electrodes (modified after Van Nostrand and Cook, 1966 [22], in Stummer, 2003 [23]).

distances between electrodes, it is called the geometric factor. It depends only on the relative distribution of electrodes. Finally, on rearranging Equation (14) we obtain:

$$\rho = K \frac{\Delta U}{I} . \quad (15)$$

For an inhomogeneous earth, this equation will produce values that vary according to the geometrical arrangement of electrodes on the surface. Values obtained from Equation (15) for an inhomogeneous underground are referred to as apparent resistivities ρ_a .

2.2. Field Survey

In this research work, geoelectric survey involving the vertical electrical sounding (VES) was carried out at 4 stations within the study area. The Schlumberger electrode array having a maximum current electrode spacing (AB) of 1362 m was used. Ninety five (95) dc electrical resistivity soundings were conducted using Terrameter SAS 300C connected to a SAS 2000 Booster. A half current electrode (AB/2) spacing ranging from 1m to 681 m was employed at each sounding location except for VES two which ranges from 1 m to 464 m. The city map showing the various sounding positions is presented as **Figure 2**. In the Schlumberger array method used in this study, the electrodes were arranged in such a way that the current electrodes (AB) were spaced farther apart than the potential electrodes (MN) as recommended by Kunetz [24]. The potential electrodes were kept constant was changed only when the voltage reading became too small to be accommodated by the instrument sensitivity. Sounding was performed by taking measurements each time the outer current electrodes were moved further apart so that the current penetrates deeper into the ground. The outer electrodes of the Schlumberger array are usually moved in steps which are approximately or accurately logarithmic. In this field measurement, the outer electrodes were moved six points to a decade in all the sounding stations and the geometric factor k used is:

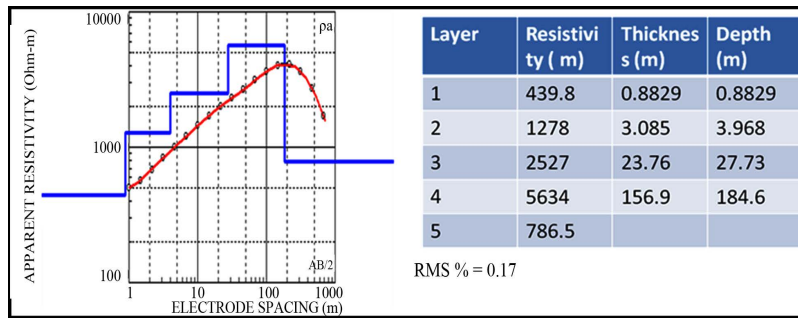
$$k = \pi \left[\frac{a^2}{b} - \frac{b}{4} \right]$$

where “ a ” is the distance between the midpoint and electrode A or B and “ b ” is the distance between M and N.

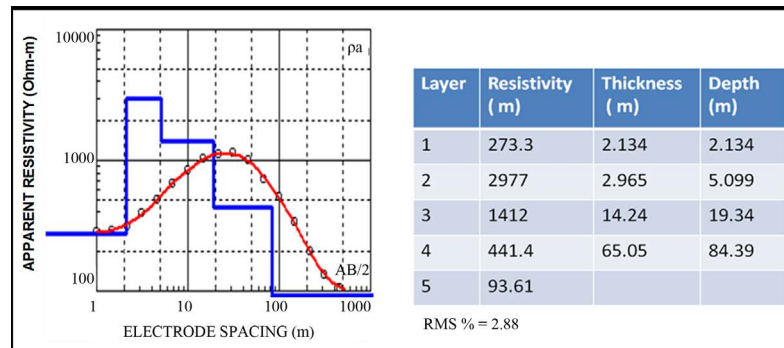
The acquired VES data were presented as sounding curves. The curves were quantitatively interpreted by partial curve matching using two layer model curves and the corresponding auxiliary curves [20]. Theoretical VES curves were generated from the partial curve matching interpretation results using the IPI2Win computer program developed by the Geophysics team of the Moscow State University [25].

3. Results and Discussions

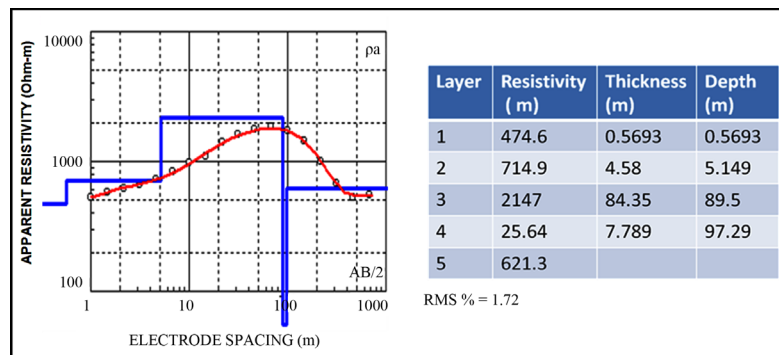
The results of the study were presented as computer plots, model parameters, geoelectric sections, geologic log and iso-resistivity maps. The field curves obtained from the study is presented as shown in **Figure 4**, which gives a best-fit interpretation of five-layer geoelectric stratification for all the VES established in Issele-Azagba. The curve types observed from the study area are AK, AKQ, and AKH. The AK curve started with a steady rise into a dome shape, followed by a discernable fall at the far end of the curve. The AKQ curves display a gradual rise from the left into a dome shape in the central section followed by the steady fall at the far right of the curve indicating an entrance into a low resistivity geoelectric zone. The AKH curves ends with a gradual rise at the far right.



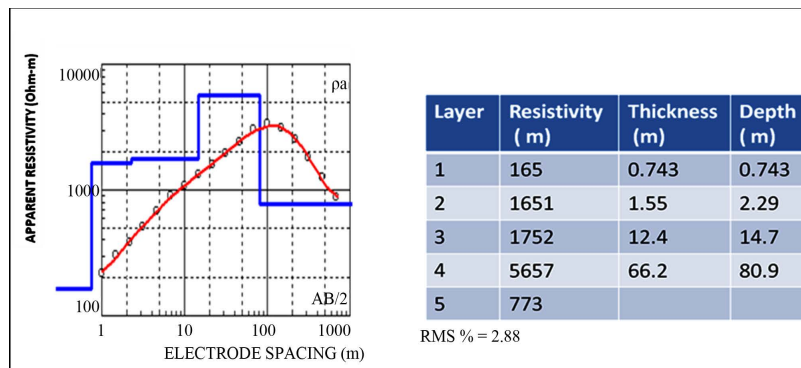
(a)



(b)



(c)



(d)

Figure 4. (a) Response Curve and Model interpretation of Issele-Azagba VES 1; (b) Response Curve and Model interpretation of Issele-Azagba VES 2; (c) Response Curve and Model interpretation of Issele-Azagba VES 3; (d) Response Curve and Model interpretation of Issele-Azagba VES 4.

The geoelectric section shown in **Figure 5** suggests that the topmost layer whose resistivity values range from 165 - 474.6 Ωm and a thickness which ranges from 0.57 - 2.13 m depicts loamy topsoil. The topsoil is underlain by geoelectric layers 2, 3 and 4 which is interpreted as an extended sandy unit of increasing compaction and wetness. The resistivity ranges from 441.4 - 5657 Ωm . This sandy horizon is very thick with a depth of about 185 m and thins out in VES 4 with a depth of about 81 m. Only in VES 3 does layer 4 depict a clayey horizon with resistivity value of 25.64 Ωm and a thickness of 7.79 m (**Figure 4(c)**).

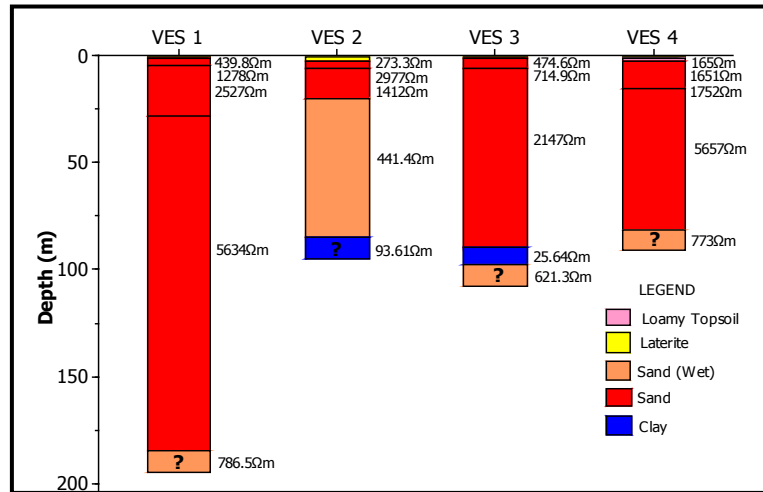


Figure 5. Geoelectric Section of Issele-Azagba VES.

The fifth substratum of the geoelectric section is interpreted as the aquiferous sand in all the VES positions except VES 2. It has a resistivity which ranges from 621.3 - 786.5 Ωm and is referred to as hydrogeologically prolific. The fifth layer in VES 2 suggests clay with a resistivity of 93.61 Ωm (**Figure 4(b)**).

Figure 6 shows the iso-resistivity map of the study area at different depths of 5 m, 10 m, 30 m, and 50 m. It indicates the extensive sandstone unit at different depth of the area with resistivity ranging from 441.4 Ωm to 5657 Ωm .

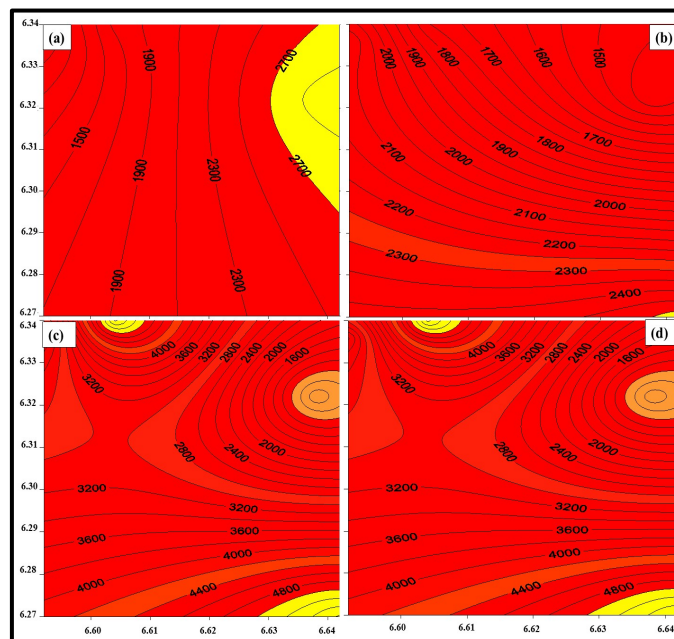


Figure 6. Iso-resistivity Map of Issele-Azagba VES: (a) = 5 m; (b) = 10 m; (c) =30 m; (d) = 50 m.

The log of two boreholes around the study area was used to correlate the VES interpretation. The logging (Figure 7) shows a lateritic topsoil underlain by a thin layer of sandy clay and clay which is overlain by a fine-medium-coarse sandstone. The borehole logs correlate well with the geoelectric records.

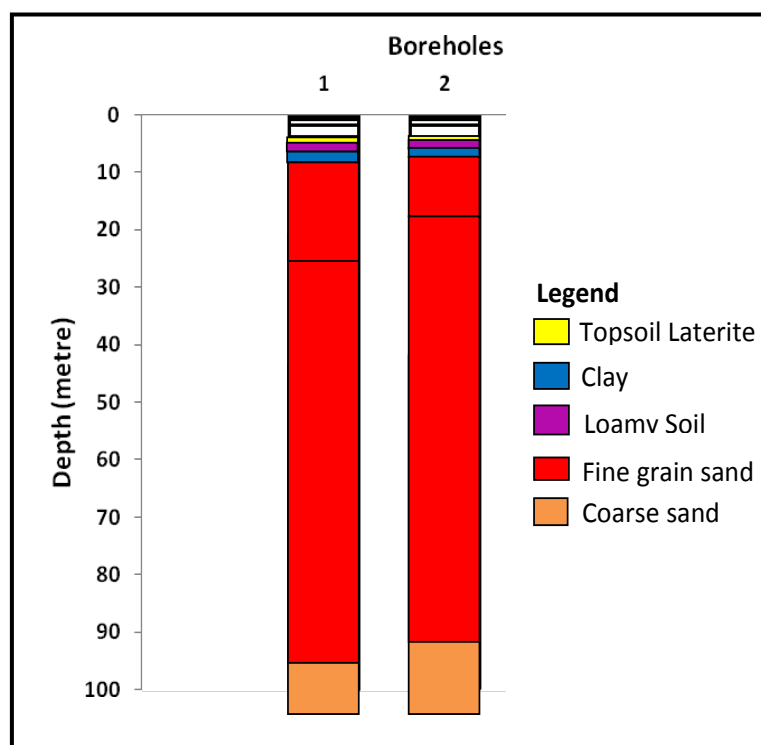


Figure 7. Litholog of Issele-Azagba Borehole.

4. Conclusion

Geophysical survey involving vertical electrical sounding technique has been carried out to delineate the subsurface formation at Issele-Azagba. The result of the survey has revealed that the subsurface geologic material in the study area is mainly loamy topsoil underlain by a relatively continuous sandy unit. The top lithologies are relatively dry with a downward increase in wetness cumulating in a semi-infinite basal unit of relatively low re-sistivity which is considered to correspond to the aquiferous unit. The depth to water table is above 100 m and varies laterally based on the topography of the area. Based on the results of the survey, the exploration and exploitation of groundwater in Issele-Azagbais are encouraging. It is therefore recommended that boreholes for sustainable water supply within the study area be drilled in excess of 100 m. The study reveals the absence of thick clay layers overlying the aquifer units hence the aquifer systems is not protected from any likely contaminants percolating from the surface. This study also reveals a better understanding of the soil properties that control the geophysical responses in this region and will thus aid in groundwater development within the study area.

Acknowledgements

This work is supported by Delta State University, Abraka, Nigeria. The author is especially thankful to Dr. Joseph Obirai of Ortrun US, LLC for his contributions and comments

References

- [1] Nobes, D.C. (1996) Troubled Waters: Environmental Applications of Electrical and Electromagnetic Methods. *Surveys in Geophysics*, **17**, 393-454. <http://dx.doi.org/10.1007/BF01901640>
- [2] Israil, M. and Pachauri, A. K. (2003) Geophysical Characterization of a Landslide Site in the Himalayan Foothill Region. *Journal of Asian Earth Sciences*, **22**, 253-263. [http://dx.doi.org/10.1016/S1367-9120\(03\)00063-4](http://dx.doi.org/10.1016/S1367-9120(03)00063-4)

- [3] Verma, R.K., Rao, M.K. and Rao, C.V. (1980) Resistivity Investigations for Ground Water in Metamorphic Areas near Dhanbad, India. *Ground Water*, **18**, 46-55. <http://dx.doi.org/10.1111/j.1745-6584.1980.tb03370.x>
- [4] Jackson, P. (1975) An Electrical-Resistivity Method for Evaluating the *in Situ* Porosity of Clean Marine Sands. *Marine Geotechnology*, **1**, 91-115. <http://dx.doi.org/10.1080/10641197509388156>
- [5] Jackson, P.D., Smith, D.T. and Stanford, P.N. (1978) Resistivity-Porosity-Particle Shape Relationship for Marine Sands. *Geophysics*, **43**, 1250-1268. <http://dx.doi.org/10.1190/1.1440891>
- [6] Fakue, M., Minato, T., Horibe, H. and Taya, N. (1999) The Micro Structures of Clay Given by Resistivity Measurements. *Engineering Geology*, **54**, 43-53. [http://dx.doi.org/10.1016/S0013-7952\(99\)00060-5](http://dx.doi.org/10.1016/S0013-7952(99)00060-5)
- [7] Park, S. and Kim, J. (2005) Geological Survey by Electrical Resistivity Prospecting in Landslide Area. *Geosystem Engineering*, **8**, 35-42. <http://dx.doi.org/10.1080/12269328.2005.10541234>
- [8] Waxman, M.H. and Smits, L.J.M. (1968) Electrical Conductivities in Oil-Bearing Shaly Sands. *Society of Petroleum Engineers Journal*, **8**, 107-122. <http://dx.doi.org/10.2118/1863-A>
- [9] Salem, H.S. (2001) The Influence of Clay Conductivity on Electric Measurement of Glacial Aquifers. *Energy Sources*, **23**, 225-234. <http://dx.doi.org/10.1080/00908310151133906>
- [10] Baines, D., Smith, D.G., Froese, D.G., Bauman, P. and Nimeck, G. (2002) Electrical Resistivity Ground Imaging (ERGI): A New Tool for Mapping the Lithology and Geometry of Channel-Belts and Valley Fills. *Sedimentology*, **49**, 444-449. <http://dx.doi.org/10.1046/j.1365-3091.2002.00453.x>
- [11] Samouelian, A., Cousin, I., Tabbagh, A., Bruand, A. and Richard, G. (2005) Electrical Resistivity Survey in Soil Science: A Review. *Soil & Tillage Research*, **83**, 173-193. <http://dx.doi.org/10.1016/j.still.2004.10.004>
- [12] Akintorinwa, O.J. and Adesoji, J.I. (2009) Application of Geological and Geotechnical Investigation in Engineering Site Evaluation. *International Journal of Physical Sciences*, **4**, 443-454.
- [13] Nwachukwu, S.O. (1972) The Tectonic Evolution of the Southern Portion of the Benue Trough, Nigeria. *Geological Magazine*, **109**, 411-419. <http://dx.doi.org/10.1017/S0016756800039790>
- [14] Olade, M.A. (1975) Evolution of the Nigeria's Benue Trough (Aulacogen): A Tectonic Model. *Geological Magazine*, **112**, 575-583. <http://dx.doi.org/10.1017/S001675680003898X>
- [15] Reymont, R.A. (1965) Aspects of Geology of Nigeria. University of Ibadan Press, Ibadan, 145.
- [16] Benkhelil, J. (1989) The Origin and Evolution of the Cretaceous Benue Trough (Nigeria). *Journal of African Earth Sciences (and the Middle East)*, **8**, 251-282. [http://dx.doi.org/10.1016/S0899-5362\(89\)80028-4](http://dx.doi.org/10.1016/S0899-5362(89)80028-4)
- [17] Kogbe, C.A. (1976) Paleogeographic History of Nigeria from Albian Times. In: Kogbe, C.A., Ed., *Geology of Nigeria*, Elizabethan Publishers, Lagos, 237-252.
- [18] Jan Du Chene, R., Onyike, M.S. and Sowumi, M.A. (1978) Some New Eocene Pollen of the Ogwahi-Asaba Formation, Southeastern Nigeria. *Revisita Espafiola de Micropaleontologia*, **10**, 285-322.
- [19] Ogala, J.E. (2012) The Geochemistry of Lignite from the Neogene Ogwashi-Asaba Formation, Niger Delta Basin, Southern Nigeria. *Earth Sciences Research Journal*, **16**, 69-82.
- [20] Keller, G.V. and Frischnecht, F.C. (1966) *Electrical Methods in Geophysical Prospecting*. Pergamon Press, New York, 519.
- [21] Cheng, K., Simske, S.J., Isaacson, D., Newell, J.C. and Gisser, D.G. (1990) Errors Due to Measuring Voltage on Current-Carrying Electrodes, in *Electric Current Computed Tomography*. *IEEE Transactions on Medical Imaging*, **37**, 60-65.
- [22] Van Nostrand, R.G. and Cook, K.L. (1966) *Interpretation of Resistivity Data*. United States Government Printing Office, Washington.
- [23] Stummer, P. (2003) *New Developments in Electrical Resistivity Imaging*. A Dissertation Submitted to the Swiss Federal Institute of Technology Zurich for the Degree of Doctor of Natural Sciences Diss Eth No 15035.
- [24] KUNETZ, G. (1966) *Principles of Direct Current Resistivity Prospecting*. Gebrüder Borntraeger, Berlin-Nikolassee.
- [25] Alexei, A.B., Igor, N.M. and Vladimir, A.S. (2001) *IPI2Win User's Guide*. Version 2.1, Geoscan-M Ltd., Moscow.

Scientific Research Publishing (SCIRP) is one of the largest Open Access journal publishers. It is currently publishing more than 200 open access, online, peer-reviewed journals covering a wide range of academic disciplines. SCIRP serves the worldwide academic communities and contributes to the progress and application of science with its publication.

Other selected journals from SCIRP are listed as below. Submit your manuscript to us via either submit@scirp.org or [Online Submission Portal](#).

